Activatable imaging probes with amplified fluorescent signals

Seulki Lee, Kyeongsoon Park, Kwangmeyung Kim, Kuiwon Choi and Ick Chan Kwon*

Received (in Cambridge, UK) 22nd April 2008, Accepted 11th June 2008
First published as an Advance Article on the web 25th July 2008
DOI: 10.1039/b806854m

Current optical imaging probe applications are hampered by poor sensitivity and specificity to the target, but molecular-level fluorescent signal activation strategies can efficiently overcome these limitations. Recent interdisciplinary research that couples the imaging sciences to fluorophore, peptide, polymer, and inorganic-based chemistry has generated novel imaging probes that exhibit high sensitivity and low background noise in both *in vitro* and *in vivo* applications. This feature article introduces and discusses the various approaches described by the term ''fluorescent signal activation methods'' with respect to their unique imaging probe design strategies and applications.

1. Introduction

Fluorescence optical imaging technologies are now paving the way for powerful analytical methods not only *in vitro*, but also *in vivo*. Cellular imaging, immunohistology, and biological enzyme assays utilize traditional fluorescence-based techniques, and since most conventional fluorescence-based probes display only modest fluorescent changes, insufficient resolution becomes the foremost limiting factor in these applications. Generally speaking, this limitation is a product of low fluorescent signal amplification and poor specificity of the imaging probe for the molecules or events of interest. Therefore, strategies that amplify the fluorescent signal or boost specific target recognition properties drive the development of highly-sensitive fluorescence-based imaging probes. Recently-developed optical imaging instruments and more sophisticated probes have expanded fluorescence-based imaging techniques, allowing researchers to detect and monitor molecular targets in live cells *in vitro* and *in vivo*, or to sense specific environmental changes in real-time.

Progress in the field of optical imaging is becoming more and more dependent on the development of novel imaging probes. As such, combining fluorophores and materials such as peptides, polymers, and novel metals has profoundly impacted the pool of available imaging probes and has significantly improved the performance of several novel optical imaging systems. Several comprehensive review articles have summarized these recent advances and have discussed their application to different strategies in the field of optical imaging.[1–3] In contrast, the present feature article summarizes the most recent reports on fluorescent imaging probes that were designed based on fluorescent signal activation. These ''activatable probes'' allow the researcher to control and manipulate fluorescence output signals by altering the chemical environment. Herein, we discuss the unique concepts, properties, and applications of the various activatable imaging probes available today.

Biomedical Research Center, Korea Institute of Science and Technology, 39-1 Hawolgok-dong, Seongbuk-gu, Seoul, 136-791, Korea. E-mail: ikwon@kist.re.kr; Fax: +82-2-958-5909; Tel: +82-2-958-5912

Ick Chan Kwon

Dr Ick Chan Kwon completed his PhD studies in pharmaceutics and pharmaceutical chemistry at the University of Utah in 1993. After post-doctoral training in the Center for Controlled Chemical Delivery at the University of Utah, he joined the Korea Institute of Science and Technology (KIST) in 1994. He is currently Head of the Biomedical Research Center at KIST and a president of the Korean Society of Molecular Imaging. He also serves as an Associate Editor of the Journal of Controlled Release, Asian Editor of the Journal of Biomedical Nanotechnology and a member of several editorial boards. His main research interest is targeted drug delivery with polymeric nanoparticles which is now expanding to the development of smart nano-probes for theragnostic imaging. He has published over 120 peer-reviewed papers and 11 book chapters, and has also given over 60 national as well as international invited lectures.

2. Fluorescent amplified imaging probes

When a dye absorbs a photon, the dye becomes electronically excited; the radiative transition from the lowest excited singlet state results in fluorescent output. In contrast, this energy can also be nonradiatively transferred between a donor (dye) and an acceptor (dye or quencher) to prevent this photon emission, thereby quenching the fluorescence. The acceptor nonradiatively absorbs the emitted photon or its associated energy from the excited donor, depending on the spectral properties of both molecules and, notably, the distance between them. This physical energy transfer process is called fluorescence resonance energy transfer (FRET).[4] The FRET process is strongly dependent on the distance between donor and acceptor (R), falling off at a rate corresponding to the sixth power of R;

therefore, FRET provides highly accurate inter- or intramolecular measurements over fairly large distances (up to 10 nm).[5] FRET is used in a broad range of applications, including estimation of protein–protein or protein–DNA interactions.[6] Additionally, in both *in vitro* and *in vivo* applications, fluorescence that has been quenched by FRET can be restored, and this manipulated fluorescence can reveal information regarding the nature of the target. In this way, quenched fluorescent FRET probes can report specific events, if they are designed such that FRET restores fluorescence that is quenched in the native state.

Choosing specific fluorophores for FRET-based imaging probes based on their respective excitation and emission ranges can provide a mechanism to differentiate between experimental conditions in *in vitro* and *in vivo* applications. Fluorophores with distinct emission spectra around 400 nm [*e.g.* 7-amino-4-methylcoumarin (AMC)], 500 nm [fluorescein isothiocyanate (FITC)], and 600 nm [5-carboxytetramethylrhodamine (TAMRA)] are widely used for *in vitro* imaging. For *in vivo* applications, however, fluorophores in the visible range have a significant drawback: visible light penetration is hampered by tissue autofluorescence and light-absorbing components such as haemoglobin, deoxyhemoglobin (max. abs. 560 nm), and water. In contrast, near-infrared (NIR) light can travel into and out of tissues more efficiently than visible light; therefore, fluorophores that operate in the NIR spectrum (650 to 900 nm) are preferable for *in vivo* imaging applications.[7]

Most of these NIR fluorophores are structurally similar to indocyanine green (ICG), a tricarbocyanine dye that is FDA-approved for clinical ophthalmic retinal angiography, cardiac function, and liver function testing. A number of NIR cyanine dyes have been synthesized, and a few of them are commercially available; *e.g.* Cy5.5 (Amersham) and Alexa 680 (Molecular Probes). Their physicochemical properties and applications for fluorescence imaging have been summarized elsewhere.[1–3] The remainder of this section discusses recently-developed, highly-sensitive FRET-based imaging probes that combine various fluorophores with peptides, polymers, and inorganic molecules to more accurately detect and image target biomolecules or specific environmental changes.

2.1 Peptide-based probes

Two peptide-based probe designs prevail, and they differ with regard to the type of quenchers used. The first strategy relies on a self-quenching mechanism, in which the donor and acceptor are the same or similar fluorophore molecules. These probes have the advantage of a less complicated synthesis, but they generally exhibit less efficient fluorescent quenching. The second strategy uses an acceptor molecule that is distinct from the donor, matching the donor fluorophore with the most efficient quencher. This design offers the advantage of high quenching efficiency but increases the complexity of the synthetic process. Activatable peptide-based probes consist of a dye and a quencher attached to opposite ends of a peptide linker. These probes are activated by target biomolecule-induced cleavage or recognition, which generates an amplified fluorescence signal by increasing the physical distance between the dye and the quencher (Fig. 1). In this section, we focus on recently-developed peptide-based probes that target unique cellular and metabolic markers in intracellular and *in vivo* systems.

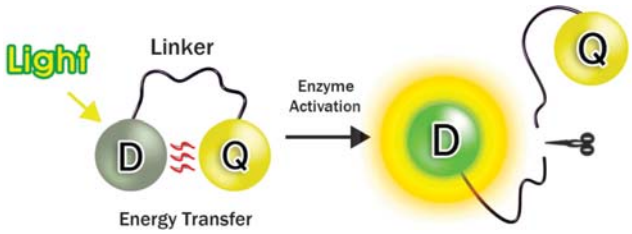

Fig. 1 Simple schematic diagram of optically activatable probes. D: Dye, Q: Quencher.

Until recently, the majority of activatable peptide-based probes targeted proteases, enzymes that hydrolyze specific peptide bonds within proteins. Proteases are overactive in a number of pathologies; these enzymes or their inhibitors have been implicated in cancer, inflammation, vascular disease, and Alzheimer's disease, as well as infectious diseases such as AIDS, Ebola, and malaria.[8,9] To better understand the onset and progression of these diseases, it is critical to identify which proteases degrade where, when, and under what physiological conditions. Sensitive, convenient, and accurate protease detection systems constitute crucial tools not only to investigate the underlying mechanisms behind these diseases, but also to improve patient treatment and prognosis. For example, drug screening systems used to identify compounds that target proteases, in addition to early diagnosis methodology for diseases such as cancer, could benefit from protease detection systems.

Many approaches utilize peptide chemistry to visualize protease activities. Most peptide-based probes detect their targets by restoring fluorescence that is quenched in the native state. The simplest and most conventional of these peptide-based probes connect the fluorophore and quencher with a protease-specific peptide spacer. This probe is optically silent in its quenched (native) state, but it becomes highly fluorescent following proteolysis of the protease substrate linker by the target enzymes. The peptide linkers are usually possible protease enzyme substrates or their family members; Table 1 summarizes several examples of peptide substrates that can be applied to detect and image various disease-associated target enzymes. Several activatable peptide-based probes that simply contain various fluorophores and/or quenchers will not be discussed herein, because they have been extensively reviewed elsewhere.[1]

Cancer imaging applications that target extracellular proteases (*e.g.*, cathepsins and MMPs) are limited by their delocalized extracellular readout. To clarify, activatable probes that target extracellular proteases are cleaved and activated nearby the cancer cells instead of within them. Therefore, the resulting fluorescence signals spread out from the cleavage site, leading to decreased signal strength. This problem can be skirted by using cell-permeable extracellular probes; *i.e.*, probes that are selectively activated near cancer cells and transported into the cells only after cell-specific activation.

Tsien and colleagues developed such a strategy for selectively delivering molecules to tumor cells based on an activatable cell-penetrating peptides (ACPPs) system.[10] In this

Table 1 Disease associated target proteases and related peptide substrates

Disease	Target protease	Peptide substrate/ cleavage site
Cancer	MMP-2/9	PLG/LR
Atherosclerosis	MMP-7	VPLS/LTM
Rheumatoid arthritis	MMP-13	PLG/MRG
	Cathepsins B	K/K
	Cathepsins D	PICF/FRL
	PSA	HSSLQ/
Apoptosis	Capspase-1	WEHD/
	Caspase-3	DEVD/
Cardiovascular	Thrombin	F(Pip)R/S
	Fijian	NQ/EQVS
Diabetes	DPP-IV	GP/GP
HIV protease	HSV	GVSQNY/PIVG

strategy, the ACPPs were composed of two strands, a Cy5-conjugated polycation (Arg; CPPs-Cy5) and a polyanion (Glu). These domains were bridged by a MMP-cleavable peptide linker (Pro-Leu-Gly-Leu-Arg-Gly). Fusing the CPPs to cleavable polyanionic sequences linkers, which neutralize the CPPs-Cy5 polycations by electrostatic interaction, effectively blocked their intracellular uptake in the absence of MMPs; subsequent cleavage of the linker by MMPs dissociated the inhibitory polyanions, leaving the CPPs-Cy5 free to be internalized. *In vivo*, these ACPPs probes successfully identified tumors overexpressing MMP-2 and -9[10] and prostate cancer cells with elevated prostate-specific antigen (PSA) expression.[11] Although this particular ACPP system did not incorporate an additional contrast mechanism, such as a fluorescence quencher, the authors did mention in their articles that adding a quencher to the end of the polyanion would efficiently improve contrast by suppressing fluorescence in the absence of the target protease (Fig. 2).

In contrast to quenched peptide-based probes that become fluorescent after specific cleavage of the peptide by proteases, Boygo and colleagues developed quenched activity-based

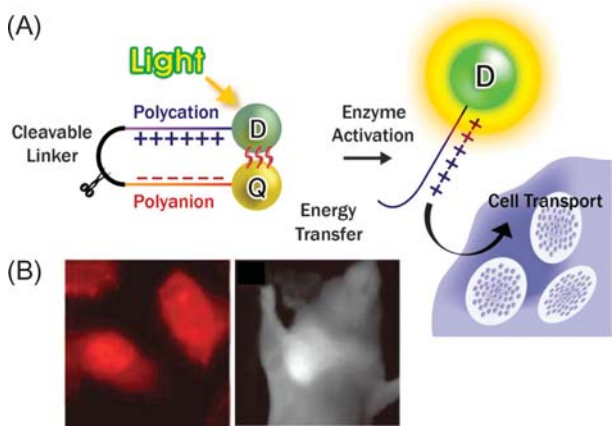

Fig. 2 (A) Schematic diagram of ACPPs. (B) Fluorescence cellular imaging of MMP-2 positive HT-1080 cells incubated with MMP-2 targetable ACCP (left). HT-1080 tumor xenografts visualized with ACCP (right). HT-1080 tumors were implanted into the mammary fat pad of nude mice and a live anesthetized animal was imaged 50 min after intravenous injection with ACCP. Fig. 2(B) is reprinted with permission from ref. 10. Copyright 2004, PNAS.

probes (qABPs) which becomes fluorescent only after labelling by active proteases (Fig. 3).[12–14] They designed and synthesized qABPs that contained a fluorescence donor and acceptor in close proximity, and hence were not fluorescent in their native state. When the qABPs encountered their target enzyme, activity-dependent covalent modification released the fluorescence acceptor, causing the probe to fluoresce brightly.

These qABPs were cell-penetrable, permitting sensitive labeling of active cysteine proteases within living cells. They then assessed the fluorescently-labeled proteases through fluorescence microscopy or standard biochemical methods.[12] Furthermore, by using quenched near-infrared fluorescent ABPs (qNIRF-ABPs), they were able to directly monitor cathepsin activity *in vivo* in mice bearing grafted tumors after intravenous injection.[14] These qNIRF-ABPs allowed for real-time imaging of target proteases, as well as secondary *ex vivo* biochemical profiling that identified specific proteases and correlated their activity with the whole body images.

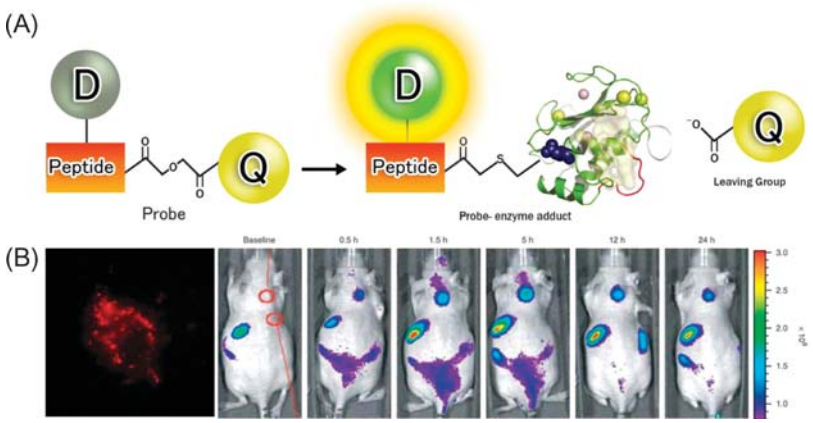

Fig. 3 (A) Schematic diagram of qABPs. (B) Imaging protease activity in live NIH-3T3 cells treated with GB117 (left, ref. 12) and serial *in vivo* near-infrared optical imaging of MDA-MB 231 MFP tumor xenografted mice after intravenous injection of ABP, GB137 (right, ref. 14). Fig. 3(B) is adapted by permission from Macmillan Publishers Ltd. Nat. Chem. Biol. (refs. 12 and 14), copyright 2005 and 2007.

Apoptosis, a programmed cell death process in multicellular organisms, plays a key role in the pathogenesis of many disorders: autoimmune and neurodegenerative disorders, cardiovascular disease, and tumor responses to chemotherapy or radiotherapy.[15] Because the majority of effective anticancer therapies initiate apoptosis, non-invasive methods to detect the progression of apoptosis could clinically assist in determining whether a patient's chemotherapy or radiotherapy regimen is working appropriately.[16] Recent reports have described a variety of activatable peptide-based probes specific for caspases, crucial mediators of apoptosis.[17] Pham *et al.* synthesized a caspase-3-activatable peptide-based probe by directly anchoring a synthesized nonfluorescent azulene quencher (abs. 750 nm) to the N-terminus of a caspase-3 cleavable peptide substrate (Asp-Glu-Val-Asp) paired with Alexa Fluor 680.[18] Treatment with caspase-3 induced a substantial increase in the fluorescent signal (greater than four-fold), but the probe was limited to use in buffered systems due to low resolution and cell membrane impermeability.

To image apoptosis in cell culture and *in vivo*, Bullok *et al.* developed a peptide-based, cell-permeable, caspase-activatable NIRF probe, TcapQ647.[19,20] TcapQ647 paired a D-amino acid, Tat-peptide-based permeation peptide sequence (Ac-arg-lys-lys-arg-arg-pyl-arg-arg-arg) to allow cell permeation, with an L-amino acid-based caspase recognition substrate (Asp-Glu-Val-Asp). Addition of a far-red quencher (QSY 21) and a fluorophore (Alexa Fluor 6470) strongly quenched the cleavable caspase-specific substrate. Recombinant enzyme assays indicated that TcapQ647 was preferentially cleaved by the effector caspases, caspase-3 and caspase-7, up to 170-fold more efficiently than the initiator caspase 9. Incorporation of a quenched fluorescence strategy onto the cell-permeable caspase substrate resulted in amplified fluorescence signals in apoptotic cells treated with the anti-cancer drug doxorubicin (Dox). Furthermore, *in vivo* experiments with TcapQ647 detected parasite-induced apoptosis in human colon xenograft and liver abscess mouse models.

Protein kinases are enzymes that catalyze phosphorylation, the transfer of a phosphate group from adenosine triphosphate (ATP) to target peptides or proteins, generating adenosine diphosphate (ADP) in the process.[21] Protein kinases play pivotal regulatory roles in most cell communication and metabolic pathways. Therefore, biochemical studies on protein kinases not only promote the characterization of signaling pathways, but they also further clinical pharmacology studies designed to develop therapeutic agents for many diseases, especially cancer. Shults and Imperiali reported the first example of a peptide-based fluorescent probe for protein kinase activity.[22,23] They designed a protein kinase-specific peptide substrate: an amino acid target sequence from Sox that generated a chelation-enhanced fluorescence signal upon binding Mg^{2+}, coupled to a phosphate moiety that acted as a metal chelator upon phosphorylation. Phosphorylation of the probe by serine/threonine protein kinases activated the Mg^{2+} chelator, thereby enhancing the fluorescent signal of the attached fluorophore (the photophysical properties of which were perturbed by interacting Mg^{2+}) by as much as five-fold.

Sharma *et al.* described a fluorescently-responsive protein kinase peptide probe employing environmentally-sensitive and

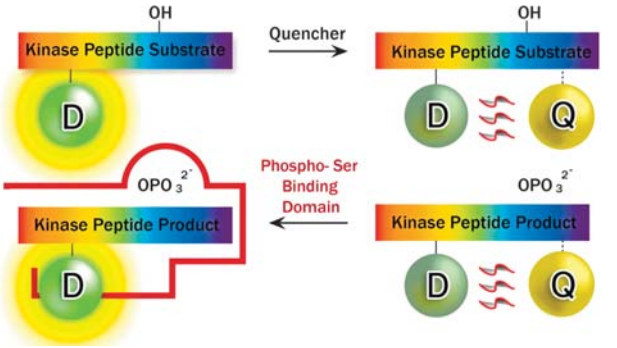

Fig. 4 Schematic diagram of deeply quenched kinase peptide substrate for sensing of protein kinase activity. Modified with permission from ref. 24. Copyright 2007, American Chemical Society.

deep-quench sensor systems (Fig. 4).[24,25] They synthesized pyrene fluorophore-conjugated protein kinase substrates, and they quenched their fluorescence by incorporating quencher molecules such as Rose Bengal, Aniline Blue WS, and Ponceau S. Under certain concentrations, the peptide and the quencher formed stable complexes in solution, most likely due to electrostatic and hydrophobic interactions. Upon phosphorylation, however, the phospho-Ser-containing peptide was sequestered by a phospho-Ser binding protein, 14-3-3τ, allowing complexes to form. Complexation disrupted the interaction between the peptide fluorophore and the quencher, generating a seven-fold enhancement of fluorescence signal intensity. The systems described above demonstrate several new approaches for amplifying fluorescent signals in protein kinase activity-specific probes; however, these approaches have not yet been conducted in an intracellular system.

Peptide-based probes have a number of advantages; for example, well-established solid-phase peptide chemistry permits custom synthesis of reproducible constructs with accurate chemical structures and facilitates modification, scale-up synthesis, handling, and storage. However, peptide-based probes often lack cell permeability, have short *in vivo* half-lives, and are not easily targeted to a region of interest; *e.g.*, tumors. Peptides can be rendered cell permeable by conjugating them to cell-penetrating peptides. These probes can also be specifically targeted to a particular cell or region by attaching short ligands that are specific for various receptors. Additionally, the *in vivo* half-lives of peptide-based probes can be significantly improved by modifying the peptides with biocompatible polymers (*e.g.*, poly(ethylene glycol) (PEG),[26] proteins, *i.e.* albumin,[27] and nanoparticles[28]) The next section describes the different design strategies behind various activatable imaging probes.

2.2 Polymer-based probes

A significant number of small molecules, including peptides, have been directly labeled with a wide range of fluorophore and/or quencher moieties by conventional chemistry, in order to use these molecules as imaging probes. Many of these probes reportedly show promising results *in vitro* and *in vivo*; however, low-molecular weight imaging probes tend to be nonspecific, unstable, and rapidly cleared. More importantly, small molecules generally lack sites permitted for chemical

modification without significanly affecting their biological activities.

Modern polymer chemistry and imaging science have yielded new strategies for designing polymer-based imaging probes that efficiently detect target molecules or diagnose diseases.[29] Polymer-based imaging probes have large surface areas (ideal for efficient modification with a wide range of imaging moieties), prolonged plasma half-lives, enhanced stability, improved targeting, and reduced nonspecific binding. Recent developments in polymer chemistry have yielded a significant number of biocompatible polymer structures, including poly(amino acids) and dendrimers, multivalent, branched, graft, and block-co-polymers. In this section, we discuss a number of innovative polymer-based imaging probes that could not have been generated by conventional peptide-based approaches.

To efficiently detect an intracellular target enzyme *in vivo*, a fluorescent probe must avoid rapid clearance and be transported out of the blood vessels to the region of interest; *e.g.*, a tumor. The most widely-applied polymer-based probes that overcome these barriers stem from probes developed by Weissleder and colleagues. This group introduced the first polymer-based imaging probe utilizing dye–dye self-quenching with an enzymatically cleavable polymer backbone.[30] The probe utilized methoxy-PEG-protected poly-L-lysine (PLL) co-polymer (PGC) as a backbone, to which Cy5.5 dye molecules were conjugated, either directly or through a protease-cleavable peptide substrate. This PGC backbone functioned *in vivo* as a long-circulating delivery carrier that could accumulate in tumors through slow leakage across their permeabilized vasculature. The backbone also served as a site for Cy5.5 or peptide–Cy5.5 attachment that was close enough to permit FRET induced by dye–dye quenching. This probe, in which Cy5.5 was directly conjugated to PGC, utilized unmodified lysine groups on the PGC as cleavage sites for enzymes such as cathepsin B (CaB) and trypsin, both of which are specific for Lys–Lys pairs.

The self-quenched probe showed a 15-fold lower fluorescence signal than the free Cy5.5 dye at equimolar concentrations, but a 12-fold higher fluorescence signal than the free dye in the presence of target enzymes. Serial fluorescent images in tumor-bearing mice demonstrated that this probe detected breast tumors[31] and other CaB overexpressing diseases, such as rheumatoid arthritis[32,33] and atherosclerosis.[34] A similar strategy utilized a near-infrared dye conjugated to an enzyme-specific peptide substrate. This probe, consisting of a peptide substrate introduced between the lysine backbone and Cy5.5, successfully imaged various proteases *in vivo*: cathepsin D,[35] MMP-2[36] and caspase-1[37] (Fig. 5). Although these PGC-based probes produced remarkably promising *in vivo* imaging results, several disadvantages limit this approach. Even though the PEG conjugated to the probe efficiently increased the stability of the probe and allowed for longer *in vivo* circulation, the PEG might also interfere with the interaction between the peptide substrate and target enzyme, based on its strong steric hindrance effect;[26] such interference could markedly decrease the sensitivity of the probe. In addition, tightly conjugating Cy5.5 dyes to the PGC backbone might increase their quenching efficiency, but they might not be cleaved as efficiently by the target proteases.

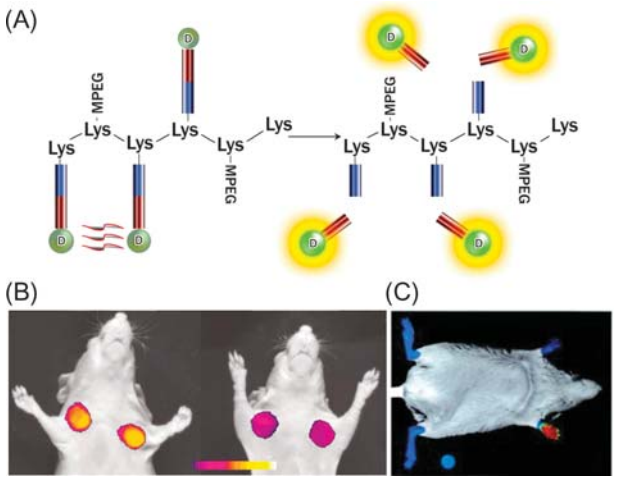

Fig. 5 (A) Schematic diagram of protease activatable PGC-based probes. *In vivo* near-infrared optical imaging of (B) MMP-2 positive HT-1080 tumor-bearing mice and (C) a mouse of collagen-induced arthritis in the right fore paw after intravenous injection of PGC-based probes. Fig. 5(B) is adapted by permission from Macmillan Publishers Ltd: Nat. Med. (ref. 36), copyright 2004. Fig. 5(C) is reprinted with permission from ref. 33. Copyright 2004, Wiley-Liss, Inc., a subsidiary of John Wiley & Sons, Inc.

As mentioned previously, a real-time imaging system for apoptosis, the programmed cell death that occurs during successful anticancer therapy, would assist in clinically managing cancer patients by revealing whether their anti-cancer therapeutic approach was working.[15] Our group developed biocompatible, NIR fluorescent-activatable polymeric nanoparticles that detected early signs of apoptosis (Fig. 6).[38] Specifically, we created apoptosis-sensitive nanoparticles by conjugating Cy5.5-Asp-Glu-Val-Asp-Cys, a caspase-3-cleavable NIR fluorescent dye-peptide substrate, to biocompatible polymeric nanoparticles (PEI-DOCA) prepared from a hydrophilic polymer [branched poly(ethyleneimine)] and a hydrophobic moiety (deoxycholic acid). The resulting spherical nanoparticles displayed an 80- to 100-nm diameter and were

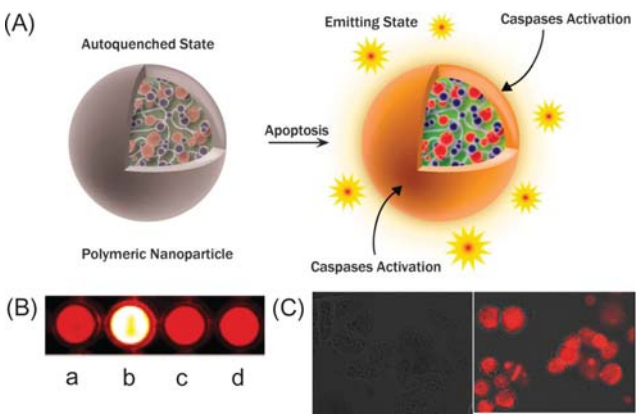

Fig. 6 (A) Schematic diagram of polymeric nanoparticles for apoptosis imaging. (B) Near-infrared fluorescence imaging of 96-well containing a. probe only, b. probe with caspase-3, c. probe with caspase-3 and inhibitor and d. scramble probe with caspase-3. (C) Fluorescence cellular imaging of HeLa cells incubated with the probe for 1 h in the presence of TRAIL, a potent inducer of apoptosis.

cell-permeable. The close spatial proximity of the Cy5.5 molecules on the polymeric nanoparticles resulted in a self-quenched state, but NIR fluorescent signals increased ten-fold in the presence of *in vitro* caspase-3. We subsequently confirmed that these polymeric nanoparticles could visualize caspase-dependent apoptosis in living cells: we treated HeLa cells preincubated with the nanoparticles with tumor necrosis factor related apoptosis-inducing ligand (TRAIL), a potent inducer of apoptosis in HeLa cells. After a one-hour treatment, all cells showed strong NIR fluorescent signals and signs of apoptosis, including apoptotic morphology. In contrast, the cells treated with control nanoparticles, containing non-cleavable scrambled peptide, did not exhibit NIR fluorescent signals, even after a two-hour treatment with TRAIL, confirming the high specificity of the autoquenched polymer nanoparticles for active caspases. In addition, Myc *et al.* demonstrated a target cell-specific poly(amidoamine) (PAMAM)-based apoptotic probe.[39] They synthesized an engineered PAMAM, generation 5, nano-device conjugated to folic acid (FA) in order to target the upregulated FA receptor in cancer cells.[40] The caspase-3 specific FRET-based agent, PhiPhiluxTM G1D1, was a conjugated apoptosis-detecting agent designed as follows: a peptide substrate for caspase-3, Gly-Asp-Glu-Val-Asp-Gly-Ile, was conjugated to two fluorophores, G1D1 (green fluorescence donor) and an acceptor. The resulting G5-Ac-FA-PhiPhiluxTM G1D1 exhibited a five-fold increase in cellular fluorescence in targeted apoptosis-induced FA-receptor-positive KB cells. Such a targeted apoptosis-detecting nano-device could simultaneously monitor delivery and apoptotic potential of a drug.

Polymeric nanoparticles have also been applied to imaging probes for protein kinase activity. Sun *et al.* reported a phosphorylation-responsive probe that utilized the polymeric micellar structure of a peptide aggregate.[41] They synthesized overall neutral-charged protein kinase-specific peptide substrates consisting of a fluorescein derivative conjugated to a fatty acid hydrocarbon tail. At high local concentrations, the probe self-assembled into micelles, promoting self-quenching of the fluorescein fluorophore. Subsequent phosphorylation increased the fluorescence intensity up to six-fold due to micellar reorganization; specifically, the negatively-charged phosphate groups disrupted the peptide aggregate by abolishing its neutral charge. Notably, this protocol is limited to cell-free conditions, because micellar structures are difficult to maintain in intracellular conditions.

While most reports conduct cell-based assays for protein phosphorylation using classical fluorescent- or radioisotope-labeled markers and bioluminescence, we recently developed a new cell-based protein kinase A (PKA) assay that applies polyion-induced biocompatible and cell-permeable polymeric nanoparticles (Fig. 7).[42–44] These polymeric nanoparticles possess a PKA-specific peptide substrate, kemptide (Leu-Arg-Ala-Ser-Leu-Gly), and are easily prepared through self-assembly of polyion-induced complexes (PIC) composed of a negatively-charged polymer, poly(aspartic acid) (PAA), and a positively-charged polymer, PEI, conjugated to Cy5.5 and kemptide.[43] The Cy5.5 dyes exhibited minimal fluorescence in the quenched state, because of the short distance between the Cy5.5 molecules in the PIC nanoparticles. Upon

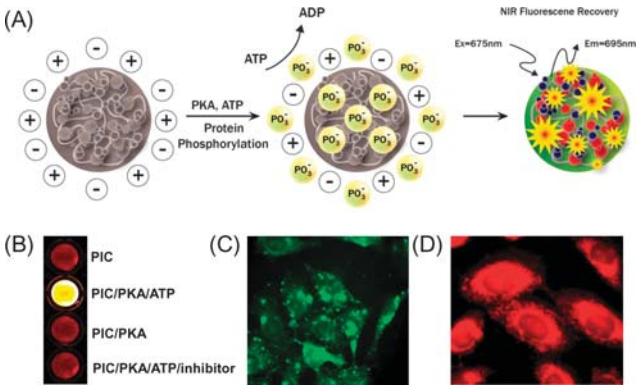

Fig. 7 (A) Schematic diagram of polymeric PIC-based imaging probes for protein kinase activity. (B) Fluorescence image from wells containing PIC nanoparticles incubated with PKA stimuli or inhibitors. (C) Cellular uptake of PIC nanoparticles incubated with the probe for 1 h. (D) Image of the probe incubated in CHO-K1 cells over expressing PKA for 1 h.

protein phosphorylation, however, the negatively-charged phosphate groups incorporated into the serine residue of the kemptide, resulting in polyelectrolyte solubilization, dissolution of the PIC nanoparticles, and rapid de-quenching of NIR fluorescent. This profound change in fluorescence, as well as their cell permeability, renders PIC nanoparticles attractive single live-cell PKA probes that do not require treatment with phosphopeptide-specific antibodies, washing steps, or genetically-modified fluorescent protein reporters.

Nonspecific interaction and labour-intensive, time-consuming protocols dominate the most commonly-employed immunoassay techniques; therefore, instantaneous identification of target molecules would vastly improve conventional immunoassay protocols. With this idea in mind, Watanabe and Ishihara developed an instantaneous bimolecular recognition assay using a FRET system engineered onto phosphatidylcholine (PC)-enriched nanoparticles (Fig. 8).[45,46] PC-group enriched surfaces are favorable for immunoassays, because the PC groups suppress nonspecific protein adsorption and stabilize immobilized biomolecules. This research group designed mono- and dual-bioconjugated nanoparticles covered with PC groups and antibodies labeled with donor (Alexa Fluor 488) and acceptor (Alexa Fluor 555) molecules to measure FRET. They selected C-reactive protein (CRP) and osteopontin (OPN), two typical target biomarkers for inflammation, as model biomolecules. As such, they conjugated CRP- or OPN-polyclonal antibodies to the fluorescence molecules and immobilized them on the PC-covered nanoparticles. Upon interaction with the target molecules (CRP or OPN), these antibody-conjugated nanoparticles formed antibody–antigen complexes, and the agglutination of nanoparticles quantitatively induced the FRET phenomenon. Their assay protocol was quite simple, and the process automatically proceeded in reaction media to provide an instantaneous, quantitative determination of target biomolecules.

Fluorescent thermometers derived from temperature-sensitive polymers can provide easy solution temperature monitoring on the basis of fluorescence emission intensity. polyNIPAM derivatives show a reversible phase transition associated with temperature-dependent hydration and

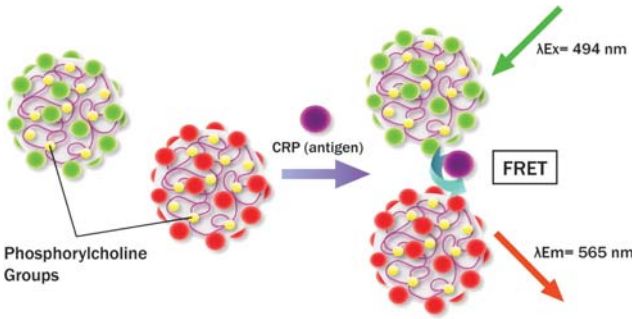

Fig. 8 Bioimaging recognition system using PC group enriched nanoparticles by FRET. Two types of nanoparticles (green and red circle: Alexa Fluor 488 and 555-labeled anti-CRP IgG, respectively) could capture the CRP antigen and FRET was then induced. Modified with permission from ref. 45. Copyright 2007, American Chemical Society.

dehydration of the polymer chain: the polymer is hydrophilic at low temperature, but as the temperature increases, it develops into polymeric aggregates through the formation of hydrophobic domains inside the polymer. Owada and colleagues designed a fluorescent thermometer based on coupling thermo-responsive random copolymers composed of an *N*-alkylamide, such as *N*-*n*-propylacrylamide (NIPAM), *N*-isopropylacrylamide (NIPMAN), or *N*-isopropylmethacrylamide (NIPMAM), to a polarity-sensitive benzofurazan that strongly emitted fluorescence in hydrophobic environments.[47–49] They showed that such fluorescent polymeric thermometers have a remarkably high temperature resolution (<0.2 °C), due to intermolecular structural changes within the polymer that greatly enhance the fluorescent emissions of polarity-sensitive dyes. Different polymer structures covered different temperature ranges with high resolution; for instance, 9–33, 30–51 or 49–66 °C. Shiraishi *et al.* reported a separate series of fluorescent thermometers that exhibited selective emission enhancement at specific temperature ranges (22–35 °C).[50]

They synthesized a simply-structured copolymer, poly(NIPAM-co-RD), consisting of NIPAM and rhodamine (RD) units as the thermo-responsive and emitting molecules, respectively. Reportedly, the fluorescence quantum yield of RD increases with the hydrophobicity of the solution. Therefore, this thermometer was based on heat-induced self-assembly of the polymer, which controls the increment and quenching of the RD emission by heat-induced increases in the hydrophobicity and size of the polymer particles (Fig. 9). Based on these strategies, fluorescent thermometers acting at different temperature ranges could easily be synthesized by changing the chemical structure of the polymer components.

Polymeric biomaterials have become increasingly important for nanobiotechnology, and all evidence suggests that their importance will continue to grow over the next few decades. Polymeric imaging probes provide researchers with potential tools to surmount many of the current limitations in conventional chemistry. Furthermore, future advances in nanobiotechnology and polymer chemistry should produce numerous structures that may lead to the development of nanosized super-sensitive smart imaging probes.

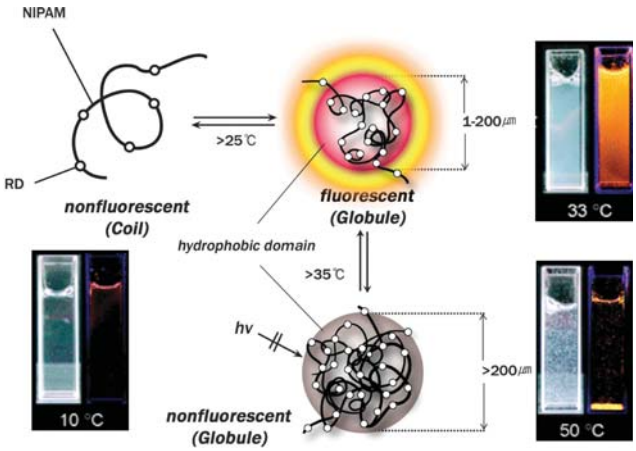

Fig. 9 Schematic diagram of the temperature-dependent changes in the structure of poly(NIPAM-co-RD). The probe behaves as a fluorescent thermometer exhibiting selective emission enhancement at a specific temperature range. Modified with permission from ref. 50. Copyright 2007, American Chemical Society.

2.3 Inorganic nanoparticle-based probes

Quantum dots (QDs) have recently generated great attention in nanobiotechnology, because their unique size-dependent, symmetric, narrow, and stable emissions allow for prolonged observation and multiplexing.[51] It is feasible that QDs might make excellent donors in FRET-based applications, because they have narrow emission and broad excitation spectra. These properties would reduce background, in that they facilitate effective separation between donor and acceptor fluorescence, and therefore widen the selection of excitation wavelengths. By placing the donor and acceptor fluorophores at precise locations on the molecules of interest, FRET measurement could generate information regarding distance and angle changes between the two fluorophores, or regarding conformational and structural changes of the labelled molecules. Until recently, applications of QD-based FRET probes as sensors have used one of the following approaches: two different-colored QDs, QD and dye-labelled proteins, QD and dye-labelled DNA, QD and gold nanoparticles, or QD and dye-labeled polymers.

Recent research has developed QD-protein assemblies as small molecular weight chemical sensors. These QD-protein assemblies were prepared by oligohistidine-mediated conjugation of a QD (λ_{max} = 560 nm) to multiple copies the of maltose binding protein (MBP) as a sugar receptor (Fig. 10).[52] In this assembly, the MBP was labeled with a β-cyclodextrin–QSY9 dark quencher conjugate (a sugar dye analogue specific for the saccharine binding pocket), which quenched QD photoluminescence (PL) by proximity-induced FRET. Exogenous maltose displaced the sugar dye analogue and manifested a concentration-dependent recovery in QD PL. Another study fabricated a chemical sensor to detect 2,4,6-trinitrotoluene (TNT), consisting of TNT-specific antibody fragments (single-chain Fv fragments, scFvs), appended with an oligohistidine sequence, immobilized on the surface of QDs.[53] Utilizing an antibody fragment instead of a full antibody substantially shortened the distance between the donor

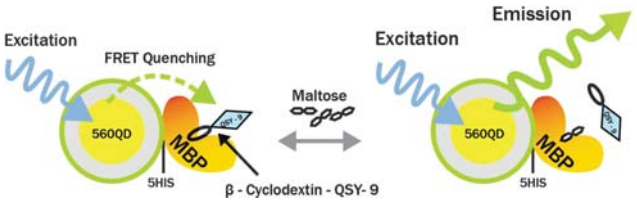

Fig. 10 Schematic diagram of self-assembled quantum dot-based nanoprobe for maltose sensing. Modified with permission from ref. 52. Copyright 2003, Nature Publishing Group.

and the antibody-bound acceptor and compacted the QD conjugate, leading to a more effective FRET process. A dye-labeled TNT analogue (TNB-BHQ-10), prebound to the scFv binding/recognition site, quenched the QD PL through proximity-induced FRET. Subsequently, exogenous TNT restored the QD PL signal in a concentration-dependent manner. This QD-based TNT sensor accurately measured TNT concentrations, within several mg L^{-1}, in unknown environment samples such as contaminated soil.

Conventional immunoassays such as ELISA require solid-phase carriers to immobilize the antibody or antigen, as well as several cycles of consecutive binding and washing to separate free and bound reagent. To overcome these limitations, some groups have applied QDs as bioanalytical immunoassay tools *in vitro*. For instance, one report described a fast and simple FRET-based sandwich fluoroimmunoassay (OsFIA) probe for detecting an antigen, using a monoclonal anti-estrogen receptor β (ER-β) labeled with QD 565 (donor) and a polyclonal anti-ER labeled with Alexa Fluor (acceptor, AF 568 or AF 633).[54] Mixing the QD-antibody and AF-antibody (1 : 3) with the ER-β antigen for 30 min induced donor quenching and acceptor enhancement of fluorescence intensity, indicating that the antibody–antigen immunocomplex had successfully formed. The QD-AF 568 immunocomplex OsFIA efficiently detected ER-β at concentrations as low as 0.05 nM. Unlike other ELISA systems, this QD-based OsFIA method did not require multiple binding, washing, and blocking steps; it might therefore be widely applicable in other immunoassays as well.

Combining imaging and therapy has led to exciting advancements in the field of nanomedicine. Bagalkot *et al*. described a multifunctional QD-based nanoparticle that detected cancer cells while simultaneously releasing anti-cancer drugs intracellularly in a reportable manner (Fig. 11).[55] In this study, the researchers designed a novel and simple proof-of-concept QD–aptamer (QD–Apt) conjugate that could concurrently deliver anticancer drugs to prostate cancer (PCa) cells and sense drug delivery based on a FRET mechanism. This QD–Apt (Dox) system was prepared by functionalizing the surface of fluorescent QDs (donor) with a targeting moiety; specifically, an aptamer that recognized the prostate-specific membrane antigen (PSMA) expressed by their model cell type (LNCaP cells). The nanoparticle was also engineered as a drug carrier by intercalating Dox into the double-stranded CG sequences of the RNA. Loading the QD–Apt with Dox rendered both the QD and Dox in the fluorescence ''OFF'' state. Upon administration, the targeted cancer cells internalized the particles and Dox was gradually released into the

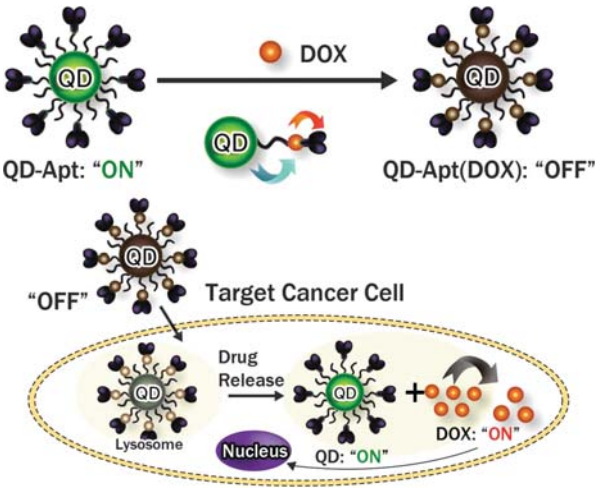

Fig. 11 Schematic illustration of Bi-FRET-based quantum dot-aptamer-doxorubicin conjugate as a targeted cancer imaging, therapy and sensing system. Reprinted with permission from ref. 55. Copyright 2007, American Chemical Society.

cells, which switched the fluorescence of the QD and Dox to the ''ON'' state. This multifunctional nanoparticle system simultaneously delivered Dox to the PSMA-expressing LNCaP cells and monitored the efficacy of Dox delivery by activating QD fluorescence. This mechanism significantly enhanced cytotoxicity and therapeutic efficacy against the targeted LNCaP cells compared to nontargeted PC3 cells. However, this QD–Apt (Dox) multifunctional nanoparticle system needed further *in vivo* studies prior to additional medical applications.

Sensitive, simple, and accurate protease-detection systems are required for the development of drug-screening systems and the early diagnosis of diseases such as cancer. Among these diverse candidates, biocompatible AuNPs have a considerable advantage in obtaining optical images *via* utilizing near-infrared fluorescence (NIRF) quenching properties.[56] It is established that chromophores in close proximity to AuNPs experience strong electronic interactions with the surface to donate excited electrons to metal nanoparticles, thus quenching fluorescence to an almost perfectly quenched state.[57] However, the use of AuNP probes in visual biomolecular detection and real-time fluorescence tomography *in vivo* remains to be explored. We recently created an alternative, simple, robust, and one-step optical fluorescence nanoprobe for use in protease inhibitor drug screening, detection of target proteases *in vitro*, and early diagnosis of cancer *in vivo* (Fig. 12).[58] We designed and prepared 20 nm gold nanoparticles which were stabilized by an N-terminally Cy5.5 labelled peptide substrate, Gly-Pro-Leu-Gly-Val-Arg-Gly-Cys, where the core specific substrate has shown selectivity for MMP-2. Glycine and cysteine were incorporated at both termini to provide the chemical conjugation sites for the Cy5.5 dyes and to functionally attach the Cy5.5 labelled substrate to AuNP surfaces using a thiol modification. The result demonstrated that the stabilized probe has strong quenching properties with minimal background signals which might allow using high concentrations of probe *in vitro* and *in vivo* without concerning the interference effect created by backgrounds. The enzyme

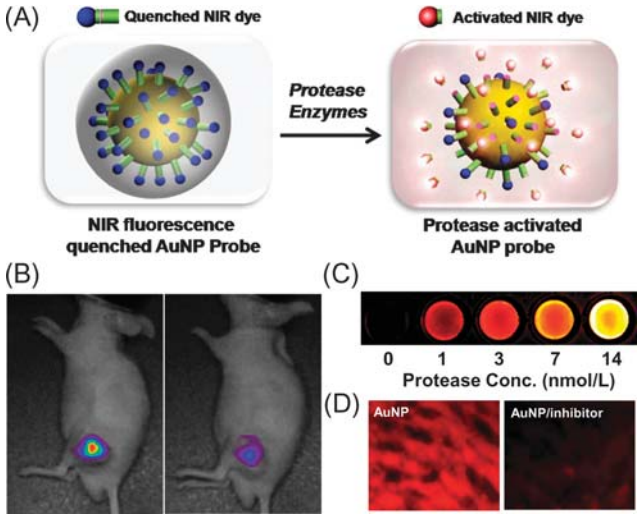

Fig. 12 (A) Schematic diagram of protease-activatable gold-quenched imaging probe. (B) *In vivo* near-infrared optical imaging of MMPs-positive SCC7 xenografts after intratumoral injection of gold probes without (left) or with (right) MMPs inhibitor. (C) Fluorescence image from wells containing the probe in the presence of various concentrations of MMP-2 following 2 h incubation. (D) Fluorescence microscopy of SCC7 tumors injected with the probe that were untreated (left) or treated (right) with inhibitor.

selectivity of the AuNP probe was evaluated *in vitro* and clearly showed that only MMPs was able to recover the potential fluorescence signals. In terms of its biocompatibility, we found that the probe is nontoxic. In addition, our result confirmed the feasibility of using AuNP probes in the detection and visualization of cancer by targeting MMP-2 *in vivo* in MMP-2 positive tumor bearing mice. This platform can be applied to any target protease by replacing the specific peptide substrate spacer between AuNP and fluorophores.

FRET has been an extremely useful tool in the sensitive determination of bioactive molecules during development of nanobiosensors. As donors, QDs have good optical characteristics and high quantum PL yields; as quenchers, AuNPs exhibit high extinction coefficients and a broad absorption spectrum within the visible light range that overlaps with the emission wavelengths of many common energy donors. For these reasons, nanobiosensors for high-sensitivity biological analyses that combine QDs (donors) with AuNPs (acceptors) have attracted increasing attention. Oh *et al.* reported an inhibition assay based on the modulation of FRET efficiency between biomolecule-conjugated QDs and AuNPs.[59] Using a streptavidin–biotin interaction, the sensing system assayed the avidin concentration in a sample solution by monitoring for PL quenching of streptavidin-conjugated QDs (SA–QDs) by biotinylated-dendrimer–AuNPs (biotin–AuNPs), as shown in Fig. 13. The biotin–AuNPs quenched the PL intensity of SA-QDs over 80%. By adding avidin, the PL intensity at 620 nm was fully recovered. This sensor could detect avidin at concentrations as low as 10 nM, based on the modulation in FRET efficiency. Similarly, QDs–ConA–β-CDs–AuNPs, uses a similar strategy to directly detect glucose in human serum

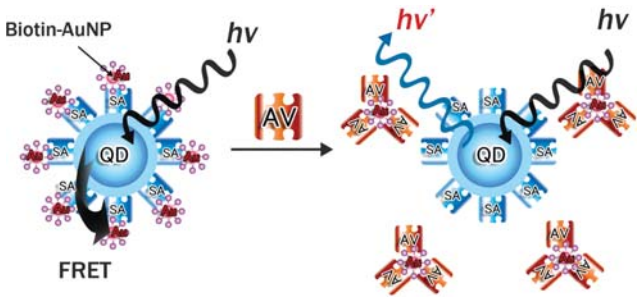

Fig. 13 Schematic diagram of inhibition assay method based on the PL quenching of SA–QDs by biotin–AuNPs. SA: streptavidin immobilized on the surface of QDs, Av: the externally added avidin. Modified with permission from ref. 59. Copyright 2006, American Chemical Society.

samples with high sensitivity and selectivity. The design of this assembled glucose nanobiosensor is based on the modulation in FRET efficiency between ConA-conjugated QDs and β-CDs-modified AuNPs. Concanavalin A (Con A), a sugar-binding lectin protein with four saccharine binding sites at pH >7.0, specifically binds glucose and mannose by a molecular recognition mechanism; β-cyclodextrins (β-CDs) have an affinity for the multivalent ConA protein. Upon adding glucose to the QDs–ConA–β-CDs–AuNPs system, the glucose competes with β-CDs for the ConA binding sites, resulting in fluorescence recovery of the quenched QDs. This sensing system is highly selective for glucose over other sugars and most biological species present in serum, and it has a detection limit as low as 50 nM. This system offers a simple, sensitive, and selective method to directly determine glucose levels in human serum.

There are numerous unexplored possibilities to expand the use of inorganic-based imaging probes. With their a unique characteristics, such as intense luminosity, high photostability and optical quenching efficacy, are one of best candidate for the multi-level imaging on both the medical and cellular bioimaging applications. However, effort is needed to avoid sample aggregation within cells and in physiological conditions, keeping their desirable optical properties intact *in vivo* and *in vitro* and optimizing imaging and detection protocols will be the key techniques to achieve. More importantly, there is an urgent need to reveal chronic toxicity and metabolism mechanisms in the body.

Conclusions

Optical imaging facilitates the integration of complex biological and physical phenomena into the rapid visualization process at a molecular level. However, current optical imaging probe applications are hampered by poor sensitivity and specificity, which innately limits their ability to image the components, processes, and dynamics of events from a molecular perspective. With the emergence of molecular-based fluorescent signal activation strategies such as those discussed herein, this limited optical resolution and specificity can be efficiently overcome. Interdisciplinary research at the interface

of the imaging sciences and peptide, polymer, and metal-based chemistry has generated novel imaging probes with highly efficient quenching and low background noise. In this feature article, we presented and introduced numerous emerging approaches enveloped by the term ''fluorescent signal activated methods,'' with respect to their imaging probe design strategies and applications. The design platforms for these imaging probes are flexible and fine-tunable for a wide array of applications, ranging from sensing environmental changes, to spot-targeting biomolecules *in vivo*, to early diagnosis of diseases such as cancer. The application of these technologies to optical imaging is still in its infancy and has a long way to go, but the improved practical potency of attractive imaging probes highlights their potential as novel tools for future imaging modalities.

Acknowledgements

This work was financially supported by the GRL Project of MEST, Intramural Research Program of the KIST and the Korea Health 21 R&D Project, Ministry of Health & Welfare, Republic of Korea (A062254).

Notes and references

1 C. H. Tung, *Biopolymers*, 2004, **76**, 391–403.
2 K. Licha and C. Olbrich, *Adv. Drug Delivery Rev.*, 2005, **57**, 1087–1108.
3 K. Stefflova, J. Chen and G. Zheng, *Front. Biosci.*, 2007, **12**, 4709–4721.
4 R. B. Sekar and A. Periasamy, *J. Cell Biol.*, 2003, **160**, 629–633.
5 P. G. Wu and L. Brand, *Anal. Biochem.*, 1994, **218**, 1–13.
6 J. Zhang, R. E. Campbell, A. Y. Ting and R. Y. Tsien, *Nat. Rev. Mol. Cell Biol.*, 2002, **3**, 906–918.
7 J. V. Frangioni, *Curr. Opin. Chem. Biol.*, 2003, **7**, 626–634.
8 M. Sajid and J. H. McKerrow, *Mol. Biochem. Parasitol.*, 2002, **120**, 1–21.
9 D. R. Edwards and G. Murphy, *Nature*, 1998, **394**, 527–528.
10 T. Jiang, E. S. Olson, Q. T. Nguyen, M. Roy, P. A. Jennings and R. Y. Tsien, *Proc. Natl. Acad. Sci. U. S. A.*, 2004, **101**, 17867–17872.
11 E. A. Goun, R. Shinde, K. W. Dehnert, A. Adams-Bond, P. A. Wender, C. H. Contag and B. L. Franc, *Bioconjugate Chem.*, 2006, **17**, 787–796.
12 G. Blum, S. R. Mullins, K. Keren, M. Fonovic, C. Jedeszko, M. J. Rice, B. F. Sloane and M. Bogyo, *Nat. Chem. Biol.*, 2005, **1**, 203–209.
13 D. Kato, K. M. Boatright, A. B. Berger, T. Nazif, G. Blum, C. Ryan, K. A. Chehade, G. S. Salvesen and M. Bogyo, *Nat. Chem. Biol.*, 2005, **1**, 33–38.
14 G. Blum, G. von Degenfeld, M. J. Merchant, H. M. Blau and M. Bogyo, *Nat. Chem. Biol.*, 2007, **3**, 668–677.
15 D. L. Vaux and S. J. Korsmeyer, *Cell*, 1999, **96**, 245–254.
16 U. Fischer and K. Schulze-Osthoff, *Pharmacol. Rev.*, 2005, **57**, 187–215.
17 Y. A. Lazebnik, S. H. Kaufmann, S. Desnoyers, G. G. Poirier and W. C. Earnshaw, *Nature*, 1994, **371**, 346–347.
18 W. Pham, R. Weissleder and C. H. Tung, *Angew. Chem., Int. Ed.*, 2002, **41**, 3659–3662, 3519.
19 K. Bullok and D. Piwnica-Worms, *J. Med. Chem.*, 2005, **48**, 5404–5407.
20 K. E. Bullok, D. Maxwell, A. H. Kesarwala, S. Gammon, J. L. Prior, M. Snow, S. Stanley and D. Piwnica-Worms, *Biochemistry*, 2007, **46**, 4055–4065.
21 M. Montminy, *Annu. Rev. Biochem.*, 1997, **66**, 807–822.
22 M. D. Shults and B. Imperiali, *J. Am. Chem. Soc.*, 2003, **125**, 14248–14249.
23 M. D. Shults, D. Carrico-Moniz and B. Imperiali, *Anal. Biochem.*, 2006, **352**, 198–207.
24 V. Sharma, R. S. Agnes and D. S. Lawrence, *J. Am. Chem. Soc.*, 2007, **129**, 2742–2743.
25 V. Sharma, Q. Wang and D. S. Lawrence, *Biochim. Biophys. Acta*, 2008, **1784**, 94–99.
26 J. M. Harris and R. B. Chess, *Nat. Rev. Drug Discovery*, 2003, **2**, 214–221.
27 J. G. Kim, L. L. Baggio, D. P. Bridon, J. P. Castaigne, M. F. Robitaille, L. Jette, C. Benquet and D. J. Drucker, *Diabetes*, 2003, **52**, 751–759.
28 M. Nahar, T. Dutta, S. Murugesan, A. Asthana, D. Mishra, V. Rajkumar, M. Tare, S. Saraf and N. K. Jain, *Crit. Rev. Ther. Drug Carrier Syst.*, 2006, **23**, 259–318.
29 J. H. Kim, K. Park, H. Y. Nam, S. Lee, K. Kim and I. C. Kwon, *Prog. Polym. Sci.*, 2007, **32**, 1031–1053.
30 R. Weissleder, C. H. Tung, U. Mahmood and A. Bogdanov, Jr, *Nat. Biotechnol.*, 1999, **17**, 375–378.
31 C. Bremer, C. H. Tung, A. Bogdanov, Jr and R. Weissleder, *Radiology*, 2002, **222**, 814–818.
32 H. Ji, K. Ohmura, U. Mahmood, D. M. Lee, F. M. Hofhuis, S. A. Boackle, K. Takahashi, V. M. Holers, M. Walport, C. Gerard, A. Ezekowitz, M. C. Carroll, M. Brenner, R. Weissleder, J. S. Verbeek, V. Duchatelle, C. Degott, C. Benoist and D. Mathis, *Immunity*, 2002, **16**, 157–168.
33 A. Wunder, C. H. Tung, U. Muller-Ladner, R. Weissleder and U. Mahmood, *Arthritis Rheum.*, 2004, **50**, 2459–2465.
34 J. Chen, C. H. Tung, U. Mahmood, V. Ntziachristos, R. Gyurko, M. C. Fishman, P. L. Huang and R. Weissleder, *Circulation*, 2002, **105**, 2766–2771.
35 C. H. Tung, S. Bredow, U. Mahmood and R. Weissleder, *Bioconjugate Chem.*, 1999, **10**, 892–896.
36 C. Bremer, C. H. Tung and R. Weissleder, *Nat. Med.*, 2001, **7**, 743–748.
37 S. M. Messerli, S. Prabhakar, Y. Tang, K. Shah, M. L. Cortes, V. Murthy, R. Weissleder, X. O. Breakefield and C. H. Tung, *Neoplasia*, 2004, **6**, 95–105.
38 K. Kim, M. Lee, H. Park, J. H. Kim, S. Kim, H. Chung, K. Choi, I. S. Kim, B. L. Seong and I. C. Kwon, *J. Am. Chem. Soc.*, 2006, **128**, 3490–3491.
39 A. Myc, I. J. Majoros, T. P. Thomas and J. R. Baker, Jr, *Biomacromolecules*, 2007, **8**, 13–18.
40 A. Quintana, E. Raczka, L. Piehler, I. Lee, A. Myc, I. Majoros, A. K. Patri, T. Thomas, J. Mule and J. R. Baker, Jr, *Pharm. Res.*, 2002, **19**, 1310–1316.
41 H. Sun, K. E. Low, S. Woo, R. L. Noble, R. J. Graham, S. S. Connaughton, M. A. Gee and L. G. Lee, *Anal. Chem.*, 2005, **77**, 2043–2049.
42 J. H. Kim, S. Lee, K. Kim, H. Jeon, R. W. Park, I. S. Kim, K. Choi and I. C. Kwon, *Chem. Commun.*, 2007, 1346–1348.
43 J. H. Kim, S. Lee, K. Park, H. Y. Nam, S. Y. Jang, I. Youn, K. Kim, H. Jeon, R. W. Park, I. S. Kim, K. Choi and I. C. Kwon, *Angew. Chem., Int. Ed.*, 2007, **46**, 5779–5782.
44 B. Schuster, *Angew. Chem., Int. Ed.*, 2007, **46**, 8744–8746.
45 J. Watanabe and K. Ishihara, *Bioconjugate Chem.*, 2007, **18**, 1811–1817.
46 J. Watanabe and K. Ishihara, *Sens. Actuators, B*, 2008, **129**, 87–93.
47 S. Uchiyama, Y. Matsumura, A. P. de Silva and K. Iwai, *Anal. Chem.*, 2003, **75**, 5926–5935.
48 C. Gota, S. Uchiyama and T. Ohwada, *Analyst*, 2007, **132**, 121–126.
49 C. Gota, S. Uchiyama, T. Yoshihara, S. Tobita and T. Ohwada, *J. Phys. Chem. B*, 2008, **112**, 2829–2836.
50 Y. Shiraishi, R. Miyamoto, X. Zhang and T. Hirai, *Org. Lett.*, 2007, **9**, 3921–3924.
51 M. Han, X. Gao, J. Z. Su and S. Nie, *Nat. Biotechnol.*, 2001, **19**, 631–635.
52 I. L. Medintz, A. R. Clapp, H. Mattoussi, E. R. Goldman, B. Fisher and J. M. Mauro, *Nat. Mater.*, 2003, **2**, 630–638.
53 E. R. Goldman, I. L. Medintz, J. L. Whitley, A. Hayhurst, A. R. Clapp, H. T. Uyeda, J. R. Deschamps, M. E. Lassman and H. Mattoussi, *J. Am. Chem. Soc.*, 2005, **127**, 6744–6751.

54 Q. Wei, M. Lee, X. Yu, E. K. Lee, G. H. Seong, J. Choo and Y. W. Cho, *Anal. Biochem*., 2006, **358**, 31–37.
55 V. Bagalkot, L. Zhang, E. Levy-Nissenbaum, S. Jon, P. W. Kantoff, R. Langer and O. C. Farokhzad, *Nano Lett*., 2007, **7**, 3065–3070.
56 E. E. Connor, J. Mwamuka, A. Gole, C. J. Murphy and M. D. Wyatt, *Small*, 2005, **1**, 325–327.
57 B. Dubertret, M. Calame and A. J. Libchaber, *Nat. Biotechnol*., 2001, **19**, 365–370.
58 S. Lee, E. J. Cha, K. Park, S. Y. Lee, J. K. Hong, I. C. Sun, S. Y. Kim, K. Choi, I. C. Kwon, K. Kim and C. H. Ahn, *Angew. Chem., Int. Ed*., 2008, **47**, 2804–2807.
59 E. Oh, M. Y. Hong, D. Lee, S. H. Nam, H. C. Yoon and H. S. Kim, *J. Am. Chem. Soc*., 2005, **127**, 3270–3271.